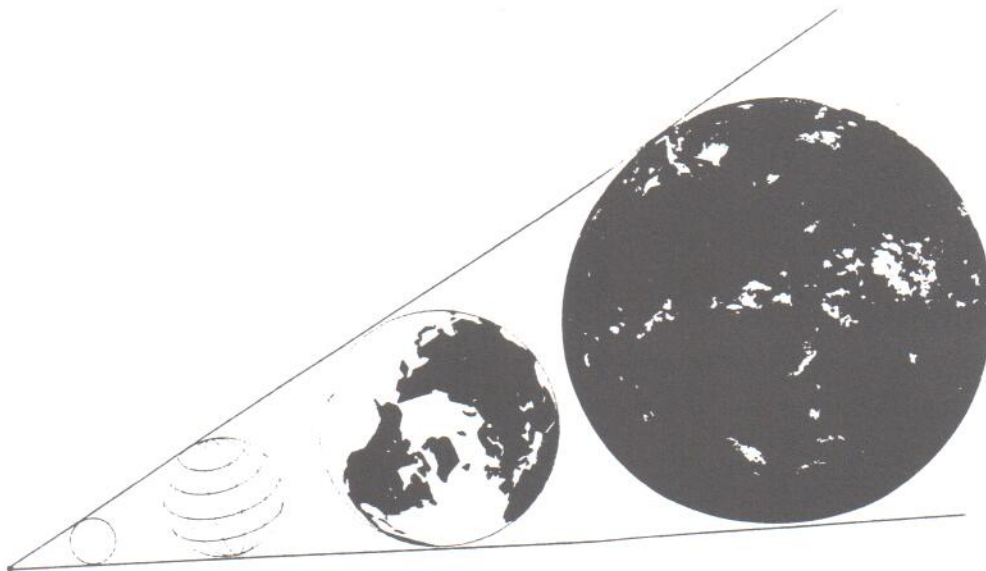


PROCEEDINGS OF THE SECOND
ACM WORKSHOP ON ADVANCES IN
GEOGRAPHIC INFORMATION SYSTEMS



December 1-2, 1994
National Institute of Standards and Technology
Gaithersburg, Maryland



EDITORS
NIKI PISSINOU
KIA MAKKI

<i>A Model to Cultivate Objects and Manipulate Fields</i>	30
G. Camara, U.M. Freitas, R.C.M. Souza, M.A. Casanova, A.S. Hemerly and C.B. Medeiros	
<i>Towards a Representation for Spatial Objects in Diverse Geometries</i>	38
J.G. Stell and M.F. Worboys	
<i>An Intersection Based Formalism For Representing Orientation Relations in a Geographic Database</i>	44
A.I. Abdelmoty and B.A. EL-Geresy	
<i>Spatial Regions with Undetermined Boundaries</i>	52
A.G. Cohn and N.M. Gotts	

Session 7: Spatial Access Structures

Chair: N. Bourbakis

<i>A Cost Model for Query Optimization Using R-Trees</i>	60
W.G. Aref and H. Samet	
<i>An Evaluation of Access Methods for Spatial Networks</i>	68
D.R. Liu, S. Shekhar and M. Coyle	
<i>Query Processing with Spatio-temporal Index on Object Oriented Databases</i>	76
C. Huang and W.S. Luk	

Session 8: Panel Session

Chair: Nick Bourbakis

<i>The Role of Multimedia and AI in GIS</i>	84
W. Campbell, B. Cheng, M. Gennert and K. Makki	

Session 9: Key-note Speech

The Mythical Map
J. Estes

Session 10: Domain Specific Requirements

Chair: C. Faloutsos

<i>Estimating Cloud Formation Evolution From Sequences of METEOSAT Images</i>	89
R. Bolla, M. Marchese, C. Nobile and S. Zappatore	
<i>A Prototype Astronomical Database</i>	95
K. Ramaiyer, R. Brunner, A. Szalay, A. Connolly and R. Lupton	

Session 11: Data Quality

Chair: P. Bergougnoux

Estimating cloud formation evolution from sequences from METEOSAT images

R. Bolla

M. Marchese

C. Nobile

S. Zappatore

*Department of Communications, Computer and System Sciences
DIST-University of Genoa
Via Opera Pia 13, 16145 Genova, Italy*

Abstract

This paper presents an algorithm to predict the short-term evolution of clouds formations with high rainfall probability by using image sequences coming from meteorological satellites (Meteosat images).

The proposed algorithm is based on four steps: the first step performs image processing procedures (thresholding and relaxation, edge following, filtering) applied to an environmental application; the second step is dedicated to the corresponding clouds problems in different images while the third deals with the complex problem of modelling the parameters defining the time evolution of a cloud formation and investigates how parameters can be estimated. The last step concerns the one or two steps forward prediction of the motion of processed clouds.

The effectiveness of the algorithm is demonstrated by experiments on real image sequences coming from Meteosat satellites.

1 INTRODUCTION

Image sequences coming from meteorological satellites are a basic means for the study of weather evolution, in conjunction with other information sources, like meteorological radars, as well as suitable models and statistical data. One of the main problems in this field is represented by the huge amount of raw data, from which the relevant information should be extracted through image processing and analysis procedures.

The framework of this work is the processing of sequences of Meteosat images in order to extract information useful in a decision support system. The goal of this latter is to describe the evolution of various cloud formations in order to foresee the rainfall probability in specific and limited areas [1].

Specifically, an algorithm is presented to estimate the evolution parameters of cloud formations characterized by high rainfall probability in a Meteosat sequence. The input to the procedure is represented by the regions of interest, extracted in two or more consecutive images by means of

suitable processing steps applied to the infrared data.

The proposed technique consists of four steps. In the first one specific image processing procedures are applied to the original images in order to extract the regions of interest in each image. Three different types of procedures are used: a first, thresholding and relaxation procedure and an edge follower are applied, then the obtained edges are filtered to detect their relevant features, thus improving the robustness of the following steps.

The second step deals with the correspondence problem between regions of interest in different images. Due to the low resolution of the Meteosat images, a texture based correlation technique cannot be used. The correspondences are therefore determined by minimizing a cost function taking into account the distance among possible regions, as well as their difference in area.

In the third step, the parameters defining the time evolution of a cloud formation are estimated. Such parameters are chosen to be those of a linear model, namely a translation vector, a rotation matrix and a deformation matrix. They are estimated by means of an iterative procedure that minimizes the not overlapping surfaces of two corresponding cloud formations.

The last step consists of using data obtained from a sequence of images to predict the evolution parameters, i.e. the centre of mass coordinates and the deformation matrix, which are used to compute the rainfall regions of the next two images in the sequence. This task is performed by employing interpolating functions, written as a linear combination of orthogonal functions, whose parameters are computed by solving a least squares problem.

The next Section describes the thresholding and relaxation procedures, and the clustering and filtering operations on the available image. In Section 3 the strategy to obtain the corresponding clouds in two consecutive images is described, while the approach to estimate the motion parameters is shown in Section 4. Section 5 presents some experimental results obtained from Meteosat imagery.

2 METEOSAT IMAGE PROCESSING

The first step of the image processing concerns thresholding and relaxation.

The goal of this step is to extract the regions characterized by high rainfall probability from a sequence of Meteosat images in the infrared band.

According with Griffith and Woodley heuristics, the regions whose temperature is below a certain threshold are

Permission to copy without fee all or part of this material is granted provided that the copies are not made or distributed for direct commercial advantage, the ACM copyright notice and the title of the publication and its date appear, and notice is given that copying is by permission of the Association of Computing Machinery. To copy otherwise, or to republish, requires a fee and/or specific permission.

CIKM'94 Workshop 12/94, Gaithersburg, MD, USA
© 1994 ACM 0-89791-750-2/94/0012...\$3.50



Figure 1: Meteosat infrared image of the 12th of June 1994, 3h am.



Figure 2: The reference image (Fig. 1), after thresholding and relaxation filtering procedure.

called clouds. In this way, the so called clouds are associated with a certain rain intensity. [2,3]

In order to improve the robustness of the thresholding procedure, a technique, based on a relaxation method, has been applied to obtain a binarized image from the original grey scale IR image.

The relaxation is, basically, a stochastic process [4,5] that allows to classify image pixels into two distinct classes (cloud points and background) by taking into account not only the pixel value but also the characteristics of the neighbouring pixels. The aim of the procedure is to correct or to reduce the inherent errors involved in classifying a point according only to its properties.

Thus the final binarized image results from removing the isolated cloud points surrounded by background points and from filling the small background areas inside a large set of cloud points.

The implemented relaxation algorithm can be sketched as follows.

- According to Griffith and Woodley law, a global threshold is determined, let it be x .
- All pixels whose values are below $x-d$ are classified as cloud points, while the pixels whose values are above $x+d$ are classified as belonging to the background, where d is a fixed number.
- All points, whose grey levels range in the $[x-d, x+d]$ interval, are assigned a probability of belonging to a cloud or to the background; this probability is iteratively updated by means of coefficients computed by using the joint probability derived from neighbour point properties.
- The iterative process stops when the point probabilities change no more within a fixed range or simply after a predefined number of runs.

At the end of the relaxation, all pixels with probability greater than 0.5 are classified as cloud points otherwise they are added to the background.

Fig. 2 shows an example of the results obtained by applying the relaxation procedure to the Meteosat image of Fig. 1 (that is called, in the following, the reference image).

Cloud points identified by the relaxation procedure need to be clustered into some connected regions (called clouds in the following). The employed clustering technique is quite simple. The binarized image is scanned from the upper left corner to the lower right one until a cloud point is encountered. Obviously this cloud point belongs to a cluster border



Figure 3: The image after the clustering procedure.

and it is used to initialize an edge follower, that operates according to the Sobel scheme reported in [6].

When the follower stops, the external cluster border is detected: the cluster is classified as a cloud if 90% otherwise the cluster is discarded. This case of bad cluster corresponds to the situation of a cloud that presents "big holes" (that is areas of background points) inside its surface.

It should be mentioned that experimental results have shown that bad cluster cases occur with low probability, once the relaxation has been performed.

The identified cluster is cancelled from the binarized image and the raster scanning is restarted till all the remaining clusters are extracted.

The clustering result is shown in Fig.3, where each cluster is represented by different grey levels.

The last operation of the image processing step is the filtering, aimed at smoothing the contours (by means of low-pass operator) obtained during the clustering; in fact, a too detailed information about the contours is not necessary for our goal and it could introduce a high computational load.

The operation is performed for each cloud contour by means of a simple monodimensional mask, sketched in Fig. 4, sliding along the boundary.

The important parameters for the low-pass filter are the mask size and the central point weight. In order to get a strong smoothing, the central point weight should be low and the mask size long enough to keep up just the shape of the edge. From a technical point of view the operation is performed on each point (x,y) of the cloud contour. For instance, by using a mask length of 5 and a central weight of F , the new value of x for the i -th point of the edge is given by the following formula:

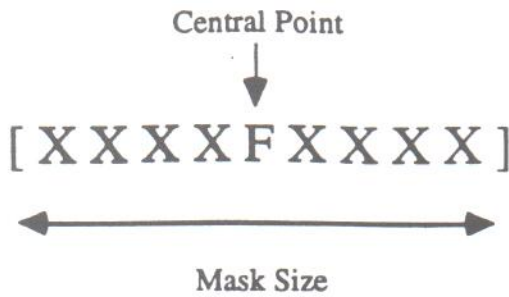


Figure 4: Mask used for the filtering operation



Figure 5: The image after filtering procedure.

$$X_{i,new} = \frac{X_{i-2,old} + X_{i-1,old} + FX_{i,old} + X_{i+1,old} + X_{i+2,old}}{F + 4} \quad (1)$$

The same technique is used to obtain the y value.

In Fig. 5, the cloud contour after the smoothing operation is depicted. It can be noted that the contour is smoothed, the detailed information is lost while the main edge shape is preserved.

3 CLOUD IDENTIFICATION

After the filtering, a crucial step is the identification of corresponding clouds in two consecutive images. A cloud in two consecutive frames can change position, orientation, scale; moreover, it can split, or join other clouds generating different cloud formations. More specifically, because of winds and atmospheric currents a cloud can split into two or more parts, thus creating other clouds not existing before; on the other hand, two or more clouds can join giving birth to one larger cloud. It can be noted that an automatic procedure detecting splitted and joined clouds is very difficult to derive.

In our approach the identification is performed in three steps: case of no splitting and joining, case of splitting, case of joining. In the first case the operation is performed by setting a variable side rectangle around the center of mass of a cloud in the first image, then by searching if some centers of mass in the second image fall inside the given rectangle; if more than one center of mass satisfies this condition a cost function is evaluated to choose the 'best' corresponding cloud. The cost function mentioned above is based on:

- the distance between centers of mass
- the difference of areas

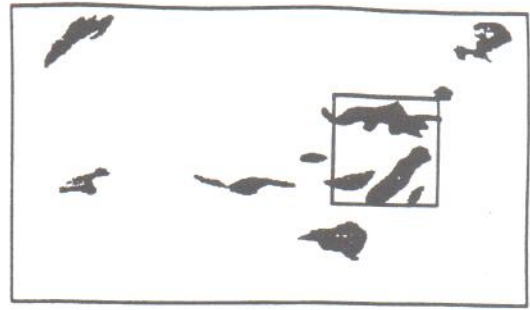


Figure 6: Identification mechanism (first image)

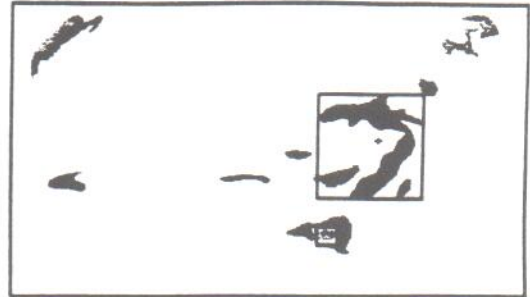


Figure 7: Identification mechanism (second image)

That is:

$$cost = \sqrt{(x_{b,j} - x_{b,i})^2 + (y_{b,j} - y_{b,i})^2} + A|Area_j - Area_i| \quad (2)$$

Being

- $x_{b,i}, x_{b,j}$ the x-values of the considered centers of mass in the first and second image, respectively
- $y_{b,i}, y_{b,j}$ the y-values of the considered centers of mass in the first and second image, respectively
- $Area_i, Area_j$ the area of the considered clouds in the first and second image, respectively

The mechanism is repeated for every cloud inside the first image; if the first step does not identify all the clouds, the case of possible splitting is investigated for not identified clouds. The operation is performed by setting a rectangle around each cloud in the first image; it is important to note that the mentioned rectangle is not set around the center of mass but it contains every point of the cloud. The second operation step is performed by examining if some centers of mass in the second image are inside the rectangle, then every possible combination for all found centers of mass is evaluated and the corresponding cloud is chosen by computing the mentioned cost function for every permutation. After finding the splitted clouds, the last operation is the evaluation of joined clusters. This step is performed by the same mechanism as in the previous case; the difference is that the rectangle is set on the second image and not on the first one.

The described mechanisms are illustrated in Fig. 6 and 7 (in a joining case), where the mentioned rectangles are drawn on real images.

4 MOTION MODELLING AND PREDICTION

Before predicting the future position of a cloud it is necessary to model the cloud motion itself.

For the sake of simplicity the motion model employed in our approach is linear, meaning that the movement of each point $\underline{x}_{i-1} = (x_i, y_i)$ of the cloud can be described [7,8] as:

$$\underline{x}_i = (\underline{d} + F\underline{x}_{i-1}) \quad (3)$$

Being:

\underline{x}_{i-1} the position of the point at instant $i-1$

\underline{x}_i the position of the point at instant i

\underline{d} the translation vector

F the shape matrix

By using the Polar Decomposition Cauchy theorem the shape matrix F can be written as the product of two matrices R and U :

$$F = RU \quad (4)$$

with $R \in O^+$ (positive definite) and $U \in Sym$ (Symmetric matrices).

From a physical point of view, the matrix R can be considered as the rotation matrix that is the matrix which contains the information about the rotation angle (q):

$$R = \begin{bmatrix} \cos \theta & \sin \theta \\ -\sin \theta & \cos \theta \end{bmatrix} \quad (5)$$

The matrix U can be interpreted as the matrix containing the information about the deformation of the cloud:

$$U = \begin{bmatrix} u_{11} & u_{12} \\ u_{12} & u_{22} \end{bmatrix} \text{ with } u_{12} = u_{21} \quad (6)$$

The problem is then reduced to the evaluation of the translation vector \underline{d} and the matrix $F = RU$. The vector \underline{d} is simply computed as the difference of the cloud centers of mass in two consecutive frames while the matrix F is evaluated by a minimization algorithm based on not overlapped surfaces. The estimated parameters associated with the motion and the deformation of a cloud during the transitions between successive frames can be exploited for an efficient prediction of the position and the shape of the cloud in the next unknown frame. The estimation of the center of mass parameters (x_b, y_b) , the rotation angle θ and the deformation matrix $U = u_{11}, u_{12}, u_{21} = u_{12}, u_{22}$ is obtained by using an interpolating function explained in the following and having as available data:

- M previous images in successive instants $(t_0, t_1, \dots, t_{M-1})$
- M values of (x_b, y_b) for each cluster
- $M-1$ values of θ for each cluster
- $M-1$ values of U for each cluster

An example of the interpolation applied to x_b with $M=3$ is shown in Fig. 8.

The succession given by the component of the cloud center of mass is interpolated by a suitable function. Once we have the analytical expression of this function we are able to determine the next coordinates of the center of mass

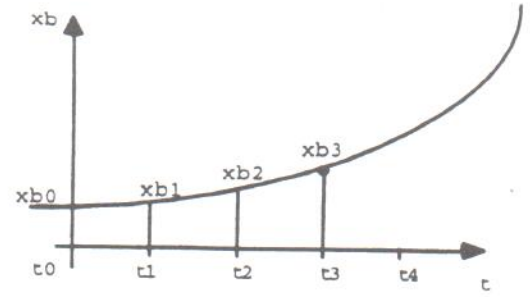


Figure 8: The interpolating function with $M=3$.

by simple substitution of the desired instant. The strategy suggested here involves the use of orthogonal functions [9] to find a good interpolation of the actual samples. Let us consider a number N of functions $p_0(t), K, p_{N-1}(t)$ defined in the interval $[0, M-1]$: these functions are said to be orthogonal in the given interval if:

$$\sum_{t=0}^{M-1} p_n(t)p_k(t) = 0 \quad (7)$$

for every $n \neq k$, and:

$$\sum_{t=0}^{M-1} p_n(t)p_n(t) = \|p_n\|^2 \quad (8)$$

if $n = k$, where $\|p_n\|^2$ is the Euclidean norm of $p_n(t)$.

We can then define an interpolating function $f(t)$ written as a linear combination of $p_0(t), K, p_{N-1}(t)$:

$$f(t) = c_0 p_0(t) + c_1 p_1(t) + L + c_{N-1} p_{N-1}(t) \quad (9)$$

in which the coefficients c_0, K, c_{N-1} are unknown and depend on the set of chosen functions and on the observed parameters. It is easy to demonstrate that:

$$c_n = \frac{\sum_{t=0}^{M-1} f(t)p_n(t)}{\|p_n\|^2} \quad (10)$$

Under the assumption that all the parameters to predict have little variations in time, we can use smooth orthogonal functions such as polynomials: this choice offers a further advantage because of the existence of a simple recursive formula to determine the desired number of functions. It can be shown that:

$$\begin{aligned} p_0(t) &= 1 \\ p_1(t) &= t - \frac{M-1}{2} \\ L & \\ p_n(t) &= p_1(t)p_{n-1}(t) - \frac{\|p_{n-1}\|^2}{\|p_{n-2}\|^2} p_{n-2}(t) \end{aligned} \quad (11)$$

If the number M of points in which these functions are defined is equal to the number N of the functions themselves, an exact solution is obtained, i.e. the function $f(t)$ exactly passes through the samples. If M is greater than N an approximate solution is obtained (Least Squares solution). Some experimental results obtained by using the presented approach are shown in the next Section.

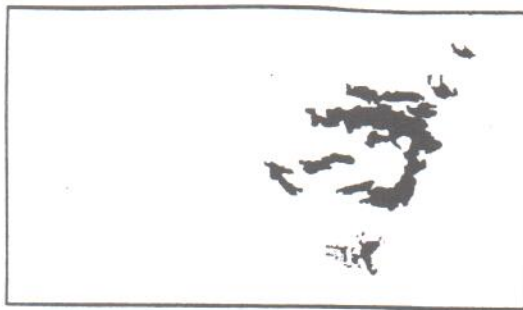


Figure 9: Clusters used in the prediction.



Figure 10: The one step predicted cluster and observed cluster of the image 4.

5 EXPERIMENTAL RESULTS

In this Section some experimental results are shown, that confirm the effectiveness of the presented prediction strategy. The prediction procedure has been applied to the sequence of three images shown in Fig. 9. The sequence contains just a cloud because the aim is to test the prediction mechanism and the presence of other clouds would have made the analysis of the results more difficult. Fig. 10 and Fig. 11 shows, respectively, the next predicted image (one step forward prediction), and the image predicted after the next (two steps forward prediction) along with the cloud shape really observed from the METEOSAT images. It can be seen that the predicted and the observed shapes are not quite different; little differences can be noted but they derive from the linear model used to describe the motion and deformation of a cloud.

In Fig. 12 the behaviour of the observed rotation angle and of the predicted one for images 3 and 4 is depicted ver-



Figure 11: Two step predicted cluster and observed cluster of the image 5.

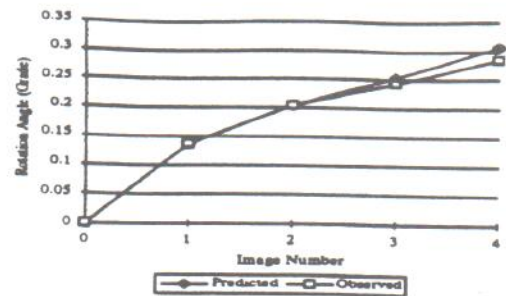


Figure 12: Behaviour of the rotation angle values and predicted angle values for image 3 and 4 versus time.

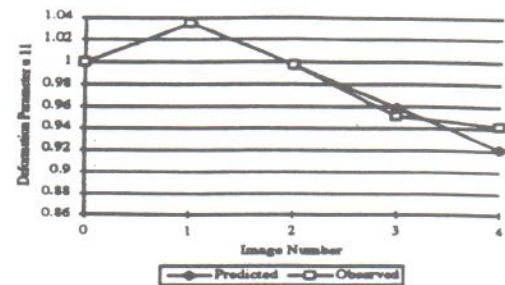


Figure 13: Behaviour of the deformation parameter u_{11} values and predicted u_{11} values for image 3 and 4 versus time.

sus time; it can be noted that the predicted value is close the observed one, especially in the one step prediction. The same consideration can be made for the behaviour of a deformation parameter (u_{11}) depicted in Fig. 13.

The results shown concern only one situation but they are representative of the average behaviour of the described prediction mechanism.

6 CONCLUSIONS

In this paper an algorithm to estimate the evolution parameters of cloud formations characterised by high rainfall probability in a Meteosat sequence has been presented. This algorithm consists of four steps: a first step, described in Section 2, of specific image processing procedures, namely a thresholding, a relaxation, an edge following and a filtering procedure, used to detect the clouds and their relevant features; a second step, described in Section 3, dealing with the correspondence problem; a third step in which the parameters defining the time evolution of a cloud formation are estimated by using a linear model and, finally, the last step in which the prediction of the evolution parameters, i.e. the centre of mass coordinates and the deformation matrix, is computed, as described in Section 4. The aim of this technique was to predict the one or two step forward evolution of the clouds by using a sequence of three or four Meteosat images. The experimental results, presented in Section 5, show that this kind of algorithm achieves this goal by providing an acceptable prediction of the first and the second forward step evolution parameter.

7 ACKNOWLEDGMENTS

This research was (in part) supported by the Commission of the European Communities, DG XII, Environment Programme, Climatology and Natural Hazard Unit, in the framework of the contract EV5V-CT0167.

8 REFERENCE

- [1] C.Braccini, G.Gambardella, A.Grattarola, S.Zappatore, "Meteosat image processing for clouds analysis and tracking", Proc. Workshop on "The role of radar in the Arno Project", Florence, Nov. 20-23, 1990.
- [2] R.F.Adeler, A.J.Negri, P.J.Wetzel, Rain Estimation from Sattelite: "An Examination of the Griffith-Woodly Technique", J. of Climate and Applied Meteorology, Vol.23,1983
- [3] G.C.Griffith, P.G.Grube, D.W.Martin, J.E.Stoud, D.N.Woodley, Rain Estimation from Geosynchronous Satellite Imagery- visible and Infrared Studies, Mon. Weather Rev. 106,1978
- [4] A.Touzani, J.G.Postaire "Mode detection by Relaxation" IEEE trans. on Pattern Anal. and Machine Intell. Vol. P.A.M.I. 10, N 6, 970-978, November 1988.
- [5] A.Rosenfeld and Russel C.Smith "Thresholding using Relaxation" IEEE trans. on Pattern Anal. and Machine Intell. Vol. P.A.M.I. 3, N 5, 588-606, September 1981.
- [6] I.Sobel, "Neighborhood coding of binary images for fast contour following and general binary array processing", Comp. Graph. Image Proc., vol.8, 1978, pp. 127-135.
- [7] S.Chadhuri and S.Chatterjee, "Motion analysis of a homogeneously deformable object using subset correspondences", Pattern Recognition, vol.24, No. 8, 1991, pp. 739-745.
- [8] D.Skea at al., "A control point matching algorithm", Pattern Recognition, vol.26, No. 2, 1993, pp. 269-276.
- [9] H.F.Harmuth, "Transmission of information by orthogonal functions", Springer- Verlag, 1969, New York, USA.